

1 **ViralLink: An integrated workflow to investigate the effect**
2 **of SARS-CoV-2 on intracellular signalling and regulatory**
3 **pathways**

4 Agatha Treveil ^{1,2}, Balazs Bohar ^{1,4}, Padhmanand Sudhakar ^{1,2,3}, Lejla Gul¹, Luca Csabai ^{1,4},
5 Marton Olbei ^{1,2}, Martina Poletti ^{1,2}, Matthew Madgwick ^{1,2}, Tahila Andrighetti ^{1,5}, Isabelle
6 Hautefort ¹, Dezso Modos ^{1,2}, Tamas Korcsmaros ^{1,2*}

7

8 ¹ Earlham Institute, Norwich, UK

9 ² Quadram Institute Bioscience, Norwich, UK

10 ³ KU Leuven Department of Chronic Diseases, Metabolism and Ageing, Translational
11 Research Center for Gastrointestinal Disorders (TARGID), Leuven, Belgium

12 ⁴ Department of Genetics, Eotvos Lorand University, Budapest, Hungary

13 ⁵ Institute of Biosciences, São Paulo University (UNESP), Botucatu 18618-689, SP, Brazil

14

15

16

17 *Corresponding author

18 Email: tamas.korcsmaros@earlham.ac.uk

19

20

21 Abstract

22 The SARS-CoV-2 pandemic of 2020 has mobilised scientists around the globe to research all
23 aspects of the coronavirus virus and its infection. For fruitful and rapid investigation of viral
24 pathomechanisms, a collaborative and interdisciplinary approach is required. Therefore, we
25 have developed ViralLink: a systems biology workflow which reconstructs and analyses
26 networks representing the effect of viruses on intracellular signalling. These networks trace
27 the flow of signal from intracellular viral proteins through their human binding proteins and
28 downstream signalling pathways, ending with transcription factors regulating genes
29 differentially expressed upon viral exposure. In this way, the workflow provides a mechanistic
30 insight from previously identified knowledge of virally infected cells. By default, the workflow
31 is set up to analyse the intracellular effects of SARS-CoV-2, requiring only transcriptomics
32 counts data as input from the user: thus, encouraging and enabling rapid multidisciplinary
33 research. However, the wide-ranging applicability and modularity of the workflow facilitates
34 customisation of viral context, *a priori* interactions and analysis methods. Through a case
35 study of SARS-CoV-2 infected bronchial/tracheal epithelial cells, we evidence the functionality
36 of the workflow and its ability to identify key pathways and proteins in the cellular response to
37 infection. The application of ViralLink to different viral infections in a cell-type specific manner
38 using different available transcriptomics datasets will uncover key mechanisms in viral
39 pathogenesis. The workflow is available on GitHub
40 (<https://github.com/korcsmarosgroup/ViralLink>) in an easily accessible Python wrapper script,
41 or as customisable modular R and Python scripts.

42 Author summary

43 Collaborative and multidisciplinary science provides increased value for experimental datasets
44 and speeds the process of discovery. Such ways of working are especially important at
45 present due to the urgency of the SARS-CoV-2 pandemic. Here, we present a systems biology
46 workflow which models the effect of viral proteins on the infected host cell, to aid collaborative
47 and multidisciplinary research. Through integration of gene expression datasets with context-
48 specific and context-agnostic molecular interaction datasets, the workflow can be easily
49 applied to different datasets as they are made available. Application to diverse SARS-CoV-2
50 datasets will increase our understanding of the mechanistic details of the infection at a cell
51 type specific level, aid drug target discovery and help explain the variety of clinical
52 manifestations of the infection.

53 Introduction

54 By mid-May 2020 at least 4000 scientific preprints and publications were released relating to
55 Severe Acute Respiratory Syndrome coronavirus 2 (SARS-CoV-2) and the disease it causes
56 (COVID-19) (Kwon 2020). This fast uptake in research efforts is vital to decrease the health
57 and economic impacts of this new pandemic. However, many questions remain unanswered
58 regarding the molecular processes driving host responses to this coronavirus. One key
59 challenge to utilisation of new findings is that published datasets are mostly unlinked to each
60 other (due to parallel efforts by multiple research groups) and not always connected to
61 community standard resources. An integrated and reusable method to interactively capture
62 new data and connect it to existing data sources is needed. Such a comprehensive approach
63 that can be run regularly when relevant new data is available, will increase and update our
64 understanding of the mechanistic details of the SARS-CoV-2 infection. Further, it will aid drug
65 target discovery by enabling identification of high confidence mediators through which the
66 virus is affecting host cells (Barabási et al. 2011). Studying the effect of the virus at molecular
67 level may explain the variety of clinical manifestations of the infection and the differences in
68 susceptibility between different populations, and together with soon available human
69 genomics data, could be used for identifying risk factors.

70

71 Upon entry of a virus into a human cell *via* surface receptors, viral RNA is released and
72 translated into proteins (Oberfeld et al. 2020). In addition to their role in direct viral replication,
73 these proteins are able to bind to human proteins creating a host-virus interface (Gordon et
74 al. 2020). This interaction can lead to downstream signalling changes in the host cell, either
75 as a result of viral hijacking or through a defined viral immune response by the host cell (Alto
76 and Orth 2012). Ultimately, this signal flow results in intracellular gene transcription changes,
77 cell-cell signalling and systemic host responses which drive the tug-of-war between the host
78 and the virus (Fung et al. 2020). In order to understand and control this conflict, it is necessary
79 to study each of these levels of host response in detail, including the intracellular response of
80 the primarily infected cell.

81

82 Currently available data relating to intracellular SARS-CoV-2 infection includes human binding
83 partners of viral proteins (Gordon et al. 2020) and transcriptomics datasets from infected cell
84 lines/organoids (Blanco-Melo et al. 2020; Lamers et al. 2020), infected patients (Liao et al.
85 2020; Huang et al. 2020) and other infected animals (Pfaender et al. 2020; Blanco-Melo et al.
86 2020). Interdisciplinary and collaborative science can maximise the value of each of these
87 datasets through data integration and comparison combined with application of different
88 computational analysis approaches. One such computational analysis method is the utilisation
89 of network approaches to model molecular interactions between the virus and human proteins

90 as well as within and between human cells (Guyen-Maiorov et al. 2017). Network approaches
91 have already been applied to study SARS-CoV-2 pathogenesis and to predict drug
92 repurposing candidates and master regulators based on proteins in proximity to human
93 binding proteins (which physically associate with SARS-CoV-2 proteins) (Gysi et al. 2020;
94 Messina et al. 2020; Zhou et al. 2020; Guzzi et al. 2020).

95

96 Here we present a systems biology workflow, to study the effect of viral infections on host
97 cells. ViralLink reconstructs and analyses a causal molecular interaction network whose signal
98 starts with the binding of an intracellular viral protein to a human protein, travels via multiple
99 signalling pathways, and ends at the transcriptional regulation of altered genes. Subsequently,
100 the workflow investigates the causal network using betweenness centrality measures, cluster
101 analysis, functional overrepresentation analysis and network visualisation. Using currently
102 available datasets from SARS-CoV-2 infected bronchial epithelial cells we demonstrate that
103 this workflow can identify biologically relevant signalling pathways and predict key proteins for
104 potential drug interventions. As the workflow is built in a modular, standardised and updateable
105 fashion, it can be used easily in the future to analyse new SARS-CoV-2 related datasets (from
106 human biopsy data, multiple tissues, etc.).

107 Methods

108 ViralLink workflow overview

109 The ViralLink workflow investigates the effect of viral infection within cells by generating and
110 analysing context-specific networks of intracellular signalling and regulatory molecular
111 interactions. These networks link the intracellular binding of viral and human proteins to the
112 transcriptional response of the infected cell (Figure 1). The context-specificity of the analysis
113 is obtained through the choice of input transcriptomics datasets - it could refer to strain of virus,
114 type of infected cell, severity of infection, age of host or any other context of interest. By
115 default, the workflow is set up to analyse the intracellular effects of SARS-CoV-2, requiring
116 only transcriptomics counts data as input and thus encouraging and enabling rapid
117 multidisciplinary research. However, the wide-ranging applicability and modularity of the
118 workflow facilitates customisation of viral context, *a priori* interactions and analysis methods.
119 ViralLink contains three primary stages: 1) collection and input of data; 2) reconstruction of
120 the network; and 3) investigation of results using functional analysis, clustering, centrality
121 measures and visualisation.

122

123

124 Collection and input of data

125 Reconstruction of causal networks using ViralLink requires four separate input datasets
126 (Figure 1): viral protein-human binding protein interactions, *a priori* human protein-protein
127 interactions (PPIs), *a priori* human transcription factor (TF) - target gene (TG) interactions and
128 an unnormalised counts matrix from a gene expression experiment. By default, all data except
129 the transcriptomics counts are provided automatically. However alternative input files can be
130 provided if desired.

131
132 The default workflow uses SARS-CoV-2 protein-human binding protein interactions obtained
133 from an affinity-purification mass spectrometry study (Gordon et al. 2020) via Intact
134 (Hermjakob et al. 2004; Orchard et al. 2014). This data was reformatted to contain one row
135 per molecular interaction with 2 columns of UniProt IDs: SARS-CoV-2 proteins and human
136 binding proteins. Alternative viral-human PPIs can be provided using the same data format.
137 The workflow assumes all viral-human interactions have an inhibiting action on the human
138 protein, unless a third column named “sign” is present in the input file containing “+” for
139 activatory and “-” for inhibitory interactions. In addition, data is provided with the workflow
140 containing the gene names corresponding to each of the SARS-CoV-2 proteins, to enable
141 easy interpretation of the reconstructed networks.

142
143 For *a priori* human interactions, the workflow obtains and uses integrated collections of PPI
144 and TF-TG interactions from OmniPath and DoRothEA, respectively (Türei et al. 2016; Garcia-
145 Alonso et al. 2019). These interactions are obtained using the ‘OmniPathR’ R package (Türei
146 et al. 2016; R Core Team 2013) to download and filter signed and directed interactions. For
147 DoRothEA, only high and medium confidence level interactions are used (confidence scores
148 A-C). In contrast to importing static input files, this script enables the use of up to date
149 interaction data. Alternative interaction data can be used with the workflow provided it has the
150 same format: specifically, it must contain source and target uniprot IDs in the columns ‘to’ and
151 ‘from’ and if the transcriptomics data uses gene symbols, the interaction data must additionally
152 contain gene symbols in the columns ‘source_genesymbol’ and ‘target_genesymbol’.
153 Furthermore, the interactions must be directed and signed with the sign of the interaction given
154 in the column ‘consensus_stimulation’ where the value ‘1’ represents a stimulation and
155 anything else represents an inhibition.

156
157 The aforementioned *a priori* interactions are contextualised using transcriptomics data from
158 any study of interest which compares viral infected to uninfected human cells or tissues.
159 Correspondingly, the workflow requires unnormalised counts data from a transcriptomics
160 experiment (containing Uniprot or gene symbols as IDs) and a corresponding mapping table

161 which lists the sample IDs (from the headers of the counts table) in the 'sample_name' column
162 and the 'test' or 'control' status of the sample in the 'condition' column. This mapping table is
163 used to carry out differential expression of a test condition (e.g. infected) compared to a control
164 condition (e.g. uninfected). An example expression dataset and mapping table are provided
165 with the workflow.

166
167 To process the transcriptomics data, the workflow uses 'DESeq2' in R to normalise the counts
168 and to carry out differential expression analysis (Love et al. 2014). Any genes passing the log2
169 fold change and adjusted p value cutoffs, based on the provided parameters (default 1 and
170 0.05, respectively), are classed as differentially expressed genes (DEGs). Following removal
171 of all genes with count = 0, normalised log2 counts across all samples are fitted to a gaussian
172 kernel (Beal 2017). All genes with expression values above mean minus three standard
173 deviations are considered as expressed genes. Subsequently, context-specific human PPI
174 and TF-TG interactions are generated by filtering only interactions where both interacting
175 molecules are expressed.

176
177 File paths to all input datasets and associated parameters (such as desired log2 fold change
178 cut off) are specified in the parameters text file which is read in by the workflow.

179 Network reconstruction

180 The reconstructed causal network contains three layers of interactions, which are obtained,
181 by default, from the three *a priori* interaction resources:

- 182 • Viral proteins interacting with human binding partners: from the SARS-CoV-2 collection
183 in the IntAct database (Hermjakob et al. 2004; Orchard et al. 2014)
- 184 • Intermediary signalling protein interactions: from protein-protein interactions (PPIs) of
185 the OmniPath collection (Türei et al. 2016)
- 186 • Transcription factors (TFs) regulating differentially expressed genes: from a
187 transcriptomics dataset of interest and the DoRothEA collection (Garcia-Alonso et al.
188 2019)

189
190 A list of all TFs targeting the differentially expressed genes are obtained from the context-
191 specific TF-TG interactions. The human binding proteins of viral proteins are connected to the
192 listed TFs through the context-specific human PPIs using a network diffusion approach called
193 Tied Diffusion Through Interacting Events (TieDIE) (Paull et al. 2013). As inputs for the TieDIE
194 tool, the following information is used: (1) The signed, directed and expression based filtered
195 PPIs is used as the input network. (2) Human proteins which are interacting partners of the
196 viral proteins are used as the start nodes. The number of viral proteins bound to each of the

197 human proteins are assigned as the weights of the start nodes. (3) The TFs of the DEGs in
198 the dataset are used as the stop nodes. The weights for each of the TFs in the set of stop
199 nodes were calculated using the following formula (Equation 1) which considers both the log2
200 fold change of the DEGs as well as the sign (i.e stimulatory or inhibitory) of the relationship
201 between the TF and the DEG.

202

$$Weight_{TF} = \frac{1}{N_{TF TG}} \sum_{n \in TG} LFC_n \cdot sign(TFTG_n)$$

203

Equation 1

$$sign(x) = \begin{cases} x = +1 & \text{if } x = \text{activatory,} \\ x = -1 & \text{if } x = \text{inhibitory.} \end{cases}$$

204

205

206 After running TieDIE, a custom R script is used to collate all the data into a final viral-initiated
207 intracellular signalling network (causal network), outputting an edge table representation of
208 the network, with a node table containing additional node annotations. Starting with the
209 interactions output from TieDIE, viral protein-human binding protein interactions are added for
210 each of the present human binding proteins. Similarly, TF-TG interactions (where the TG is a
211 DEG) are added for each of the present TFs, creating a full network with three interaction
212 types: SARS-CoV-2 protein-human binding protein, PPI and TF-DEG. All nodes of the network
213 are added to a node table with annotations including heat values (output from TieDIE), Entrez
214 IDs (obtained in R using the 'org.Hs.eg.db' package), gene symbols (obtained from UniProt
215 (UniProt Consortium 2019)) and log2 fold change values from the differential expression
216 analysis.

217 Network investigation

218 Following reconstruction of the causal network, ViralLink provides functionality to investigate
219 the results using functional analysis, clustering, centrality measures and visualisation.

220 Centrality measures

221 To identify key molecules in the reconstructed network ViralLink uses a betweenness centrality
222 measure - calculating the global importance of a node (in this case a protein) based on the
223 number of shortest paths which pass through them when connecting all node pairs in the
224 network (Koschützki and Schreiber 2008). Nodes with high betweenness centrality play a key
225 role in transduction of signals through the network, and here represent proteins with biological
226 importance in the cellular response to viral infection. Betweenness centrality is calculated for
227 each node in the causal network using the R package 'igraph' and output as an annotation in

228 the node table (Csárdi and Nepusz 2006). Alternative centrality measures are available using
229 the 'igraph' package and can be integrated into the workflow by the user if required.

230 Cluster analysis

231 Clustering algorithms are commonly used in network biology to investigate the complex
232 structure of molecular interaction networks by extracting groups of densely connected
233 molecules (Bader and Hogue 2003; Brohée et al. 2008). Depending on the number of
234 molecules included, a cluster can represent a molecular complex or a group of molecules
235 which function closely with each other. Cluster analysis can identify subsets of a large network
236 with specific functions and indicate molecules that may have functional redundancy with each
237 other - potentially having implications for drug targeting. ViralLink employs the MCODE
238 clustering method to identify groups of densely connected nodes in PPI networks (Bader and
239 Hogue 2003). To carry out this analysis, ViralLink requires a local version of the Cytoscape
240 software to be open (Shannon et al. 2003; Su et al. 2014), which is controlled programmatically
241 using the R package 'RCy3' with the Cytoscape 'MCODE' app (v1.6.1) (Gustavsen et al.
242 2019). MCODE is run using default parameters: degree cut off =2, haircut=TRUE, node score
243 cut off=0.2, k-core=2, max depth=100. This analysis outputs the data as node annotations in
244 the node table, which are used for the functional analysis and visualisation steps of the
245 workflow. If Cytoscape is not running, this step of the workflow will be skipped.

246 Functional analysis

247 To further investigate important cellular functions and signalling pathways directly affected by
248 the virus of interest, ViralLink carries out functional overrepresentation analysis on different
249 parts of the causal network:

- 250 1. The DEGs of the network
- 251 2. The upstream human proteins (including human binding proteins, intermediary
252 signalling proteins and TFs)
- 253 3. Identified clusters (only those with ≥ 15 nodes are investigated)

254
255 Functional overrepresentation analysis is carried out in R using packages 'ClusterProfiler' (for
256 Gene Ontology annotations (Ashburner et al. 2000)) and 'ReactomePA' (for Reactome
257 annotations (Yu et al. 2012; Yu and He 2016; Fabregat et al. 2018)). For analysis of the
258 upstream human signalling proteins and analysis of clusters, all proteins in the context-specific
259 human PPI interactions are used as the background. For analysis of the DEGs, all target
260 genes in the context-specific human TF-TG interactions are used as the background. For
261 Gene Ontology (Biological Process) analysis (except when running the compareCluster

262 command), the 'simplify' command is used (cutoff=0.1, select_fun=min) to remove redundant
263 functions. All functions with $q \text{ val} \leq 0.05$ are considered significantly overrepresented.

264

265 An additional R script is provided alongside the workflow which creates subnetworks of the
266 causal network based on functions of interest. These function-specific subnetworks highlight
267 how specific signalling pathways in the infected cell reach (and subsequently affect) specific
268 functions of the DEGs. For example, the subnetwork could be created to show how viral
269 proteins can affect different host toll-like receptor pathways, and how these pathways can
270 ultimately affect DEGs associated with interleukins. In this network the DEG nodes would be
271 replaced with nodes representing the interleukin functions (which must be overrepresented
272 based on the functional analysis). This script requires the output files from the functional
273 analysis, the node and edge tables of the causal network and a file of all Uniprot IDs
274 associated with all Reactome functions (which is provided with ViralLink, following download
275 from the Reactome website in April 2020). In addition, the script requires a list of
276 overrepresented DEG functions (Reactome) and a list of upstream signalling functions
277 (Reactome) to visualise. The script outputs an edge table, a node table and a Cytoscape file
278 (if Cytoscape is open locally at the time of running the script).

279 Visualisation

280 Data visualisation is often an important part of biological network interpretation, providing new
281 insights into the data and visually conveying analysis results (Pavlopoulos et al. 2008). As
282 such, ViralLink has the capability to import reconstructed networks into the open-source
283 Cytoscape network visualisation software (Shannon et al. 2003; Su et al. 2014). This
284 functionality requires that the user has Cytoscape installed and open locally. Specifically, the
285 workflow employs the 'RCy3' R package to interact with Cytoscape programmatically,
286 importing the node and edge tables to create network visualisations and saving the data as a
287 '.cys' file. The causal network, the network clusters (where containing ≥ 15 nodes) and the
288 function-specific networks are visualised in this way. If calculated previously, the causal
289 network nodes are coloured based on their betweenness centrality, however further style and
290 layout customisation must be carried out by the user directly based on the data.

291 Implementation

292 The workflow consists of modular R and Python scripts which can be run separately or through
293 the provided Python wrapper script. If running for the study of SARS-CoV-2, the only required
294 input files are related to the transcriptomics data of interest: a raw counts table (using gene
295 symbols or UniProt protein IDs) and a two-column metadata table specifying test and control
296 sample IDs. One further script is provided to generate function-specific networks. This script

297 is not included in the wrapper because it requires the user to specify functions of interest from
298 the output of the functional analysis. To run everything, it is necessary that the user has R,
299 Python3 and Cytoscape installed. The only file the user needs to edit is the parameters text
300 file where input file paths and parameters are specified. All scripts, default input files and
301 details of how to run the scripts are freely accessible on GitHub
302 (<https://github.com/korcsmarosgroup/ViralLink>).

303 Use case

304 To demonstrate the application of this workflow for the study of SARS-CoV-2, we applied it to
305 a published transcriptomics dataset. We downloaded raw counts tables from a transcriptomics
306 study of SARS-CoV-2 infected (MOI 2, 24 hour incubation) NHBE cells (Normal Human
307 Bronchial/tracheal Epithelial cell line) with uninfected controls (Blanco-Melo et al. 2020) via
308 Gene Expression Omnibus (accession GSE147507) (Edgar et al. 2002; Barrett et al. 2013).
309 OmniPath and DoRothEA (v2, A-C) were downloaded on 15/04/2020. Any genes with log₂
310 fold change $\geq |0.5|$ and adjusted p value ≤ 0.05 were classed as differentially expressed. All
311 networks were visualised in Cytoscape (v3.7.2).

312 Results

313 Use case: SARS-CoV-2 infection of lung cells

314 To demonstrate the application of this workflow for the study of SARS-CoV-2, we created
315 intracellular signalling networks of NHBE cells (from Normal Human Bronchial/tracheal
316 Epithelial cell lines) upon infection with SARS-CoV-2 based on data published by Blanco Melo
317 *et al.* (Blanco-Melo et al. 2020) and viral-human binding protein interactions published by
318 Gordon *et al.* (Gordon et al. 2020). The resulting causal network contains 804 nodes
319 (molecules) and 5423 interactions (Figure 2A, Supplementary Tables 1-2, Supplementary File
320 1). The 10 most central proteins of the reconstructed causal network (based on betweenness
321 centrality) are involved in a wide range of cellular functions (Figure 2B). Taken together these
322 proteins highlight the propensity for SARS-CoV-2 to affect cell proliferation, apoptosis, cell
323 adhesion, exocytosis and proinflammatory immune responses. These functions are influenced
324 through multiple cellular pathways, most notably MAPK/ERK and PI3K/AKT signalling
325 pathways.

326

327

328

329

330 Functional overrepresentation analysis of the causal network identified an enrichment of
331 interleukin and interferon related functions among the network DEGs, in line with previously
332 published findings (Supplementary Figure 1, Supplementary File 2) (Zhang et al. 2020; Chua
333 et al. 2020; Huang et al. 2020). Overrepresented functions and pathways of the upstream
334 signalling proteins (human binding proteins, intermediary signalling proteins and TFs) included
335 innate immunity-related functions, platelet signaling, PI3K/AKT signalling, MAPK activation,
336 estrogen receptor-mediated signalling, senescence and a number of growth factor receptor-
337 associated functions (such as VEGF signalling, receptor tyrosine kinases, stem cell growth
338 factor signalling (SCF-KIT) and neurotrophin receptor signaling). Therefore, we show that this
339 analysis highlights additional pathways through which SARS-CoV-2 could be affecting the lung
340 epithelial cells, which cannot be identified by looking at the transcriptomic results in isolation.

341

342 Based on functional overrepresentation analysis, we created a function-specific network by
343 sub setting the causal network. This visualisation was used to further explore the mechanisms
344 of how specific signalling pathways are affecting the DEGs (Supplementary Figure 2A,
345 Supplementary File 3). Specifically, we generated an innate-immunity associated subnetwork
346 containing all upstream human signalling proteins associated with Reactome functions
347 cytokine signalling in immune system, signaling by interleukins and MyD88-independent TLR4
348 cascade and all overrepresented functions of the DEGs (in place of the DEG nodes). These
349 pathways contain 9/10 of the top betweenness centrality nodes (all except RHOA), evidencing
350 the centrality and importance of the innate immune response to viral infection. Inspecting the
351 TF layer of this immune subnetwork, we find a number of key TFs including STAT proteins (3
352 and 4), IRF proteins (1 and 5) and NFkB-related proteins (NFkB1, NFkBIA).

353

354 Finally, we evidenced the application of MCODE clustering analysis to using the reconstructed
355 SARS-CoV-2-infected NHBE cell causal network. We identified four clusters containing 15 or
356 more nodes, making up 19% of the network (154/804) (Supplementary Figure 2B,
357 Supplementary Table 2, Supplementary File 1). Assuringly, 9/10 of the top betweenness
358 centrality nodes were included in these four clusters, further confirming the high connectivity
359 and importance of these nodes in the causal network. Functional overrepresentation analysis
360 of the cluster nodes highlighted a functional similarity between all four of the clusters
361 (Supplementary Figure C-D, Supplementary File 2). Likely this is due to the high number of
362 inter-cluster molecular interactions and because of the functional similarities between the top
363 central nodes.

364

365 Collectively, we show that our systems biology workflow, Virallink, reconstructs a functionally
366 relevant intracellular signalling network affected by SARS-CoV-2 infection. Investigation of the

367 networks through functional analysis, centrality measures and cluster analysis, combined with
368 network visualisations, enables detailed study of the key proteins and pathways involved in
369 signal transduction.

370 Discussion

371 Infection by SARS-CoV-2 can cause a complex and systemic response by the human body.
372 As such, a better mechanistic understanding of the effects of SARS-CoV-2 will aid
373 identification of effective drug treatments and help to explain the differences in susceptibilities
374 across different populations (Kirby 2020). This understanding can be gained using cross-
375 disciplinary approaches which combine 'omics data generation, computational systems
376 biology and validatory web lab experiments (Korcsmaros et al. 2017). Here we present a
377 computational workflow that can be used to model the cellular response to infection by
378 integrating knowledge of human binding proteins of viral proteins with the transcriptional
379 response of a cell/cell type. Whilst set up primarily to run analyses based on SARS-CoV-2,
380 ViralLink can be applied to any viral infection, provided data is available describing possible
381 interactions between the viral proteins and human proteins.

382
383 ViralLink builds on our previously published resource MicrobioLink, which reconstructs
384 networks representing the effect of extracellular and intracellular microbial proteins on cellular
385 processes (Andrighetti et al. 2020). Differing from MicrobioLink, ViralLink inputs a
386 predetermined list of viral-host PPIs and focuses only on pathways ending in transcriptional
387 regulation: thereby reducing the complexity of the workflow (for accessibility and speed
388 purposes) and increasing its predictive confidence. Furthermore, ViralLink extends the
389 functionality of MicrobioLink with more advanced network analysis (functional enrichment,
390 clustering and centrality measures) and visualisation options.

391
392 By exploiting previously collated and comprehensive collections of molecular interactions
393 (Türei et al. 2016; Garcia-Alonso et al. 2019), ViralLink predicts how signal flows from the
394 initial interaction with a viral protein or protein fragment to the ultimate transcriptional changes
395 induced by the virus. Through mapping the direct intracellular effect of viral infection (using a
396 network approach), this workflow enables further investigation into specific signalling
397 pathways and transcription factors which play a key role in signal transduction. Signalling
398 pathways are primarily regulated through post-translational modifications and thus would not
399 be identified using transcriptomics datasets (Antebi et al. 2017). In addition, the resulting
400 intracellular networks allow identification of differentially regulated genes that are affected as
401 a direct result of viral recognition by protein-protein signalling pathways, rather than by
402 secondary signals such as elevated cytokine levels. This permits a more focused analysis of
403 possible drug targets and adds to the understanding of viral pathomechanisms. Functional
404 analysis and visualisation methods included in the workflow are vital for interpretation of the
405 generated intracellular networks, enabling detailed investigation of key proteins and signalling
406 pathways.

407

408 Due to the modularity of the workflow, it can be easily adjusted or extended - different diffusion
409 and propagation algorithms, such as HotNet2 (Leiserson et al. 2015; Cowen et al. 2017), could
410 be implemented as required. The implemented diffusion tool, TieDIE, adds mechanistic value
411 by accounting for local causality (e.g. sign) but, on the other hand, has a reduced possible set
412 of input *a priori* interactions. If desired, a diffusion tool which does not need signed *a priori*
413 interactions can be implemented to increase the input dataset size. Alternatively, a different
414 method, such as an integer linear programming approach which identifies paths based on an
415 optimisation problem (as implemented in CARNIVAL), could be used for network
416 reconstruction (Liu et al. 2019). In addition, integration of CARNIVAL could extend the
417 workflow to permit network reconstruction without supplying upstream perturbations (in this
418 case the viral-host protein interactions). Whilst not currently integrated due to data availability
419 issues, the addition of phosphoproteomics data to the pathway propagation methods could
420 improve the prediction of active pathways (Dugourd et al. 2020) Alternatively, methods to
421 predict protein activity based on transcriptional signatures, such as VIPER and PROGENy
422 (Alvarez et al. 2016; Schubert et al. 2018) could be added to the workflow in addition to
423 network diffusion methods to increase the confidence of pathway predictions. Finally,
424 extension of the network to include additional regulatory molecule types (e.g. miRNAs) or to
425 study non-human hosts, could uncover further mechanisms by which SARS-CoV-2 can affect
426 host cells.

427

428 Accessible through GitHub, the workflow requires R and Python3 to be installed (and
429 Cytoscape for clustering and visualisation), however only a limited programming ability is
430 required to run the code. All code is wrapped into a Python script with a separate file where
431 all input file paths and parameters are specified. At a minimum, only two user specified input
432 files are required: a raw counts table from a transcriptomics study (using gene symbols or
433 UniProt protein IDs) and a two-column metadata table specifying test and control sample IDs.
434 All other files are provided or acquired directly within the workflow - but can be changed by
435 the user if required. However, one limitation of the current workflow is that creation of
436 Cytoscape visualisations and clustering analysis require the user to install and open the
437 Cytoscape app. If this is not possible, for example because the scripts are not being run on a
438 machine with a graphical interface, these steps are skipped. Furthermore, only basic
439 visualisation is possible programmatically, due to challenges applying one visualisation
440 strategy to all possible output networks, especially with regard to the function-based networks.

441

442 In addition to accessibility through a default emphasis on SARS-CoV-2, a key strength of this
443 workflow is the ability to use different input datasets: including different *a priori* molecular
444 interactions, viral-human binding protein interactions and expressed/differentially expressed

445 gene lists. This allows extensive customisation and permits rapid implementation to the most
446 cutting-edge data soon after publication. Running the workflow across different
447 transcriptomics datasets will allow comparison of intracellular viral responses between
448 different cell types, different species and across different conditions (such as severe vs
449 asymptomatic infection). For example, application of the workflow to transcriptomics data from
450 specific immune cell-types, such as macrophages, will likely uncover different host affected
451 signalling pathways and key TFs based on the infected cell-type. This, in turn, could increase
452 our understanding of the role of different immune populations in fighting the infection. In
453 addition, the workflow can be run on data from other SARS-CoV-2 strains when and if they
454 emerge, thereby aiding comparisons of mechanisms of action between the strains.

455

456 To evidence the use of this workflow, we applied it to study the effect of SARS-CoV-2 infection
457 in lung epithelial (NHBE) cells using transcriptomics data published by Blanco-Melo *et al.*
458 (Blanco-Melo *et al.* 2020). In the resulting causal network, DEGs directly affected by SARS-
459 CoV-2 initiated signalling are associated with functions that are known responses to SARS-
460 CoV-2 and other viral infections (Cao 2020; Shi *et al.* 2020; Sallard *et al.* 2020; Arvanitakis *et*
461 *al.* 1998). Upstream of these affected genes we identified a number of potentially important
462 signalling pathways relating to classical viral-immune responses, cell survival and cytoskeletal
463 rearrangements and cell adhesion. Previous investigation of the first SARS coronavirus
464 (SARS-CoV) identified an inhibition of cell proliferation and an increase in apoptosis regulated
465 to PI3K/AKT signalling (Mizutani *et al.* 2006; Tsoi *et al.* 2014). Our network of SARS-CoV-2-
466 initiated intracellular signalling suggests that the PI3K/AKT signalling and the AKT1 protein
467 itself are key mediators of SARS-CoV-2 initiated signal transduction and that apoptosis and
468 cell proliferation pathways are affected by SARS-CoV-2, thus highlighting similarities between
469 the two viruses. However, further experimentation and/or data curation is required to confirm
470 the direction of change of specific pathways (up- or downregulated) based on the results of
471 the presented workflow. Together our results indicate that SARS-CoV-2 can affect NHBE cells
472 through a variety of signalling pathways which have been previously associated with similar
473 viruses, including growth factor signalling, MAPK/ERK signalling and PI3K/AKT signalling.
474 Furthermore, centrality measures and cluster analysis identified proteins which likely play a
475 key role in transduction of these signals, and could be good targets for drug treatments.

476

477 Several other network reconstruction methods exist which could be and have been applied to
478 study SARS-CoV-2 infections. For example Messina *et al.* and Gysi *et al.* (Messina *et al.* 2020;
479 Gysi *et al.* 2020) use diffusion algorithms and other similar methods to investigate proteins in
480 close proximity to human binding proteins based on PPI interactions and gene co-expression
481 networks. Our workflow builds on these approaches by linking viral proteins to DEGs. Through
482 this method we can observe which signalling pathways mediate the effect of the virus on

483 cellular transcription levels, creating a systems level view of cellular changes as a result of the
484 virus. Using the functional analysis methods and network visualisation capabilities of the
485 workflow, it is possible to predict which viral proteins and host signalling pathways can affect
486 specific cellular functions, enabling more focused identification of drug targets. In addition to
487 protein mediators, this method describes TFs which are involved in the cellular response and
488 identifies which DEGs can be affected as a direct result of viral proteins hijacking host
489 signalling and which are affected through a different mechanism. In addition to the presented
490 workflow, at least one other method has been used to reconstruct SARS-CoV-2-initiated
491 intracellular signalling networks (Ding et al. 2020) corroborating the benefits of such analysis
492 methods. Differing from the here presented approach, this work uses an extended version of
493 the Signaling Dynamic Regulatory Events Miner method to reconstruct the networks, resulting
494 in a more mathematically complex but computationally heavy analysis (Gitter et al. 2013).
495 Furthermore, the workflow by Ding *et al.* is a less reusable and accessible workflow because
496 it was designed for a specific analysis.

497

498 In conclusion, ViralLink is an easily accessible, reproducible and scalable systems biology
499 workflow to reconstruct and analyse molecular interaction networks representing the effect of
500 the viruses on intracellular signalling. We believe it is the first available integrative workflow
501 for analysing the downstream effects of viral proteins using viral host interactions and host
502 response data. Application of this workflow to study COVID-19 based on a wide variety of
503 conditions and datasets will uncover mechanistic details about SARS-CoV-2 infection of
504 different cell types, providing valuable predictions for wet-lab and clinical validation.

505

506

507 Acknowledgements

508 Many thanks to members of the Saez-Rodriguez group and to the COVID-19 Disease Map
509 Community for their ideas and support. In particular we thank Julio Saez-Rodriguez, Alberto
510 Valdeolivas and Aurelien Dugourd for their advice and discussions and Nigel Fosker for help
511 with the manuscript. This research was supported in part by the NBI Computing infrastructure
512 for Science (CiS) group through the provision of a High-Performance Computing (HPC)
513 Cluster.

514

515 Funding

516 A.T., L.G., M.O., M.P. and M.M. are supported by the BBSRC Norwich Research Park
517 Biosciences Doctoral Training Partnership (grant numbers BB/M011216/1 and
518 BB/S50743X/1). The work of T.K., D.M., and I.H. was supported by the Earlham Institute
519 (Norwich, UK) in partnership with the Quadram Institute (Norwich, UK) and strategically
520 supported by the UKRI Biotechnological and Biosciences Research Council (BBSRC) UK
521 grants (BB/J004529/1, BB/P016774/1, and BB/CSP17270/1). T.K. and D.M. were also funded
522 by a BBSRC ISP grant for Gut Microbes and Health BB/R012490/1 and its constituent
523 project(s), BBS/E/F/000PR10353 and BBS/E/F/000PR10355. P.S. was supported by funding
524 from the European Research Council (ERC) under the European Union's Horizon 2020
525 research and innovation programme (grant agreement no. 694679).

526 Figure and Tables

527 **Figure 1: ViralLink workflow overview.**

528

529 **Figure 2. Causal network of SARS-CoV-2-infected NHBE cells. A)** Signalling flows from
530 left to right: SARS-CoV-2 proteins/protein fragments (red triangles), human binding proteins
531 (yellow parallelograms), intermediary signalling proteins (blue circles), transcription factors
532 (green rectangles) and differentially expressed genes (grey rhombuses). Where a human
533 protein/gene is acting in multiple layers of the network, it is only visualised once based on the
534 following priority: DEGs, binding proteins, TFs, signalling proteins. **B)** Results of betweenness
535 centrality analysis, which measures the global importance of nodes (molecules) in the network.
536 Nodes coloured based on their betweenness centrality parameter, with the gene names of the
537 10 highest scoring (most central) nodes overlaid. DEGs have \log_2 fold change $\geq |0.5|$ and
538 adjusted p value ≤ 0.05 .

539

540

541 **Supplementary Figure 1. Overrepresented Reactome functions (A, B) and Gene**
542 **Ontology Biological Processes (C, D) of the causal network of SARS-CoV-2 infected**
543 **NHBE cells. A)** Top 10 overrepresented Reactome functions of upstream signalling proteins
544 (including human binding proteins, intermediary signalling proteins and TFs) **B)** Top 10
545 overrepresented Reactome functions of network DEGs C) Top 10 overrepresented GO-BP
546 functions of upstream signalling proteins (including human binding proteins, intermediary
547 signalling proteins and TFs) D) All overrepresented GO-BP functions of network DEGs (q
548 value ≤ 0.05). DEGs have \log_2 fold change $\geq |0.5|$ and adjusted p value ≤ 0.05 .

549

550 **Supplementary Figure 2: Function-specific network SARS-CoV-2- infected NHBE cells**
551 **and cluster analysis on SARS-CoV-2-infected NHBE causal network. A)** Function-specific
552 subnetwork containing upstream signalling proteins related to the top overrepresented (q
553 value ≤ 0.05) innate immunity-related Reactome functions (cytokine signalling in immune
554 system, signaling by interleukins and MyD88-independent TLR4 cascade) and all
555 overrepresented functions of the DEGs (in place of the DEG nodes). Layers of the network
556 and node shapes same as in Figure 2. DEGs = differentially expressed genes. DEGs have
557 \log_2 fold change $\geq |0.5|$ and adjusted p value ≤ 0.05 . See Supplementary File 3. B) Cluster
558 analysis results where clusters have ≥ 15 nodes. Position of clustered proteins shown within
559 the causal network and to the right as isolated clusters. Nodes coloured by their cluster
560 membership (black=unclustered, green=cluster 1, yellow=cluster 2, pink=cluster 3,
561 blue=cluster 4). Presence of top 10 betweenness centrality nodes in the clusters is indicated
562 to the right of the clusters. B) Gene Ontology (GO) overrepresentation analysis of the clusters.

563 Top five GO terms (by adjusted p value) displayed for each cluster. **C)** Reactome
564 overrepresentation analysis of the clusters. Top five Reactome terms (by adjusted p value)
565 displayed for each cluster. See Supplementary Table 2 and Supplementary File 2.

566

567 **Supplementary Table 1: Causal network of SARS-CoV-2-infected NHBE cell.**

568

569 **Supplementary Table 2: Node annotations for causal network of SARS-CoV-2-infected**
570 **NHBE cell.** Includes betweenness centrality measures and clusters identified by MCODE.
571 MCODE clusters 1,3,4 and 5 correspond to the clusters in the manuscript labelled 1,2,3 and
572 4 respectively. Clusters 2 and 6 were excluded due to size.

573

574 **Supplementary File 1: Causal network of SARS-CoV-2-infected NHBE cell, Cytoscape**
575 **file.**

576 **Supplementary File 2: Functional overrepresentation results.** Reactome and Gene
577 Ontology Biological Processes (q value ≤ 0.05) for differentially expressed genes (DEGs),
578 protein-protein (PPI) interaction nodes (human binding proteins, signalling proteins and
579 transcription factors) and the clusters of the causal network of SARS-CoV-2-infected NHBE
580 cell.

581 **Supplementary File 3: Function-specific network of SARS-CoV-2- infected NHBE cells,**
582 **Cytoscape file.**

583 References

- 584 Alto, N.M. and Orth, K. 2012. Subversion of cell signaling by pathogens. *Cold Spring Harbor*
585 *Perspectives in Biology* 4(9), p. a006114.
- 586 Alvarez, M.J., Shen, Y., Giorgi, F.M., et al. 2016. Functional characterization of somatic
587 mutations in cancer using network-based inference of protein activity. *Nature Genetics* 48(8),
588 pp. 838–847.
- 589 Andrichetti, T., Bohar, B., Lemke, N., Sudhakar, P. and Korcsmaros, T. 2020. MicrobioLink:
590 An Integrated Computational Pipeline to Infer Functional Effects of Microbiome-Host
591 Interactions. *Cells* 9(5).
- 592 Antebi, Y.E., Nandagopal, N. and Elowitz, M.B. 2017. An operational view of intercellular
593 signaling pathways. *Current Opinion in Systems Biology* 1, pp. 16–24.
- 594 Arvanitakis, L., Geras-Raaka, E. and Gershengorn, M.C. 1998. Constitutively signaling G-
595 protein-coupled receptors and human disease. *Trends in Endocrinology and Metabolism*
596 9(1), pp. 27–31.
- 597 Ashburner, M., Ball, C.A., Blake, J.A., et al. 2000. Gene Ontology: tool for the unification of
598 biology. *Nature Genetics* 25(1), pp. 25–29.
- 599 Bader, G.D. and Hogue, C.W.V. 2003. An automated method for finding molecular
600 complexes in large protein interaction networks. *BMC Bioinformatics* 4, p. 2.
- 601 Barabási, A.-L., Gulbahce, N. and Loscalzo, J. 2011. Network medicine: a network-based
602 approach to human disease. *Nature Reviews. Genetics* 12(1), pp. 56–68.
- 603 Barrett, T., Wilhite, S.E., Ledoux, P., et al. 2013. NCBI GEO: archive for functional genomics
604 data sets--update. *Nucleic Acids Research* 41(Database issue), pp. D991-5.
- 605 Beal, J. 2017. Biochemical complexity drives log-normal variation in genetic expression.
606 *Engineering Biology* 1(1), pp. 55–60.
- 607 Blanco-Melo, D., Nilsson-Payant, B.E., Liu, W.-C., et al. 2020. Imbalanced Host Response to
608 SARS-CoV-2 Drives Development of COVID-19. *Cell* 181(5), pp. 1036-1045.e9.
- 609 Brohée, S., Faust, K., Lima-Mendez, G., Vanderstocken, G. and van Helden, J. 2008.
610 Network Analysis Tools: from biological networks to clusters and pathways. *Nature Protocols*
611 3(10), pp. 1616–1629.
- 612 Cao, X. 2020. COVID-19: immunopathology and its implications for therapy. *Nature*
613 *Reviews. Immunology* 20(5), pp. 269–270.
- 614 Chua, R.L., Lukassen, S., Trump, S., et al. 2020. Cross-talk between the airway epithelium
615 and activated immune cells defines severity in COVID-19. *medRxiv*.

- 616 Cowen, L., Ideker, T., Raphael, B.J. and Sharan, R. 2017. Network propagation: a universal
617 amplifier of genetic associations. *Nature Reviews. Genetics* 18(9), pp. 551–562.
- 618 Csárdi, G. and Nepusz, T. 2006. The igraph software package for complex network
619 research. *undefined*.
- 620 Ding, J., Lugo-Martinez, J., Yuan, Y., Kotton, D.N. and Bar-Joseph, Z. 2020. Reconstructing
621 SARS-CoV-2 response signaling and regulatory networks. *BioRxiv*.
- 622 Dugourd, A., Kuppe, C., Sciacovelli, M., et al. 2020. Causal integration of multi-omics data
623 with prior knowledge to generate mechanistic hypotheses. *BioRxiv*.
- 624 Edgar, R., Domrachev, M. and Lash, A.E. 2002. Gene Expression Omnibus: NCBI gene
625 expression and hybridization array data repository. *Nucleic Acids Research* 30(1), pp. 207–
626 210.
- 627 Fabregat, A., Jupe, S., Matthews, L., et al. 2018. The Reactome Pathway Knowledgebase.
628 *Nucleic Acids Research* 46(D1), pp. D649–D655.
- 629 Fung, S.-Y., Yuen, K.-S., Ye, Z.-W., Chan, C.-P. and Jin, D.-Y. 2020. A tug-of-war between
630 severe acute respiratory syndrome coronavirus 2 and host antiviral defence: lessons from
631 other pathogenic viruses. *Emerging microbes & infections* 9(1), pp. 558–570.
- 632 Garcia-Alonso, L., Holland, C.H., Ibrahim, M.M., Turei, D. and Saez-Rodriguez, J. 2019.
633 Benchmark and integration of resources for the estimation of human transcription factor
634 activities. *Genome Research* 29(8), pp. 1363–1375.
- 635 Gitter, A., Carmi, M., Barkai, N. and Bar-Joseph, Z. 2013. Linking the signaling cascades
636 and dynamic regulatory networks controlling stress responses. *Genome Research* 23(2), pp.
637 365–376.
- 638 Gordon, D.E., Jang, G.M., Bouhaddou, M., et al. 2020. A SARS-CoV-2 protein interaction
639 map reveals targets for drug repurposing. *Nature*.
- 640 Gustavsen, J.A., Pai, S., Isserlin, R., Demchak, B. and Pico, A.R. 2019. RCy3: Network
641 biology using Cytoscape from within R. [version 3; peer review: 3 approved].
642 *F1000Research* 8, p. 1774.
- 643 Guven-Maiorov, E., Tsai, C.-J. and Nussinov, R. 2017. Structural host-microbiota interaction
644 networks. *PLoS Computational Biology* 13(10), p. e1005579.
- 645 Guzzi, P.H., Mercatelli, D., Ceraolo, C. and Giorgi, F.M. 2020. Master Regulator Analysis of
646 the SARS-CoV-2/Human Interactome. *Journal of clinical medicine* 9(4).
- 647 Gysi, D.M., Valle, Í.D., Zitnik, M., et al. 2020. Network Medicine Framework for Identifying
648 Drug Repurposing Opportunities for COVID-19. *arXiv*.
- 649 Hermjakob, H., Montecchi-Palazzi, L., Lewington, C., et al. 2004. IntAct: an open source

- 650 molecular interaction database. *Nucleic Acids Research* 32(Database issue), pp. D452-5.
- 651 Huang, L., Shi, Y., Gong, B., et al. 2020. Blood single cell immune profiling reveals the
652 interferon-MAPK pathway mediated adaptive immune response for COVID-19. *medRxiv*.
- 653 Kirby, T. 2020. Evidence mounts on the disproportionate effect of COVID-19 on ethnic
654 minorities. *The Lancet. Respiratory medicine*.
- 655 Korcsmaros, T., Schneider, M.V. and Superti-Furga, G. 2017. Next generation of network
656 medicine: interdisciplinary signaling approaches. *Integrative Biology: Quantitative*
657 *Biosciences from Nano to Macro* 9(2), pp. 97–108.
- 658 Koschützki, D. and Schreiber, F. 2008. Centrality analysis methods for biological networks
659 and their application to gene regulatory networks. *Gene regulation and systems biology : 2*,
660 pp. 193–201.
- 661 Kwon, D. 2020. How swamped preprint servers are blocking bad coronavirus research.
662 *Nature* 581(7807), pp. 130–131.
- 663 Lamers, M.M., Beumer, J., van der Vaart, J., et al. 2020. SARS-CoV-2 productively infects
664 human gut enterocytes. *Science*.
- 665 Leiserson, M.D.M., Vandin, F., Wu, H.-T., et al. 2015. Pan-cancer network analysis identifies
666 combinations of rare somatic mutations across pathways and protein complexes. *Nature*
667 *Genetics* 47(2), pp. 106–114.
- 668 Liao, M., Liu, Y., Yuan, J., et al. 2020. The landscape of lung bronchoalveolar immune cells
669 in COVID-19 revealed by single-cell RNA sequencing. *medRxiv*.
- 670 Liu, A., Trairatphisan, P., Gjerga, E., Didangelos, A., Barratt, J. and Saez-Rodriguez, J.
671 2019. From expression footprints to causal pathways: contextualizing large signaling
672 networks with CARNIVAL. *NPJ Systems Biology and Applications* 5, p. 40.
- 673 Love, M.I., Huber, W. and Anders, S. 2014. Moderated estimation of fold change and
674 dispersion for RNA-seq data with DESeq2. *Genome Biology* 15(12), pp. 550–550.
- 675 Messina, F., Giombini, E., Agrati, C., et al. 2020. COVID-19: Viral-host interactome analyzed
676 by network based-approach model to study pathogenesis of SARS-CoV-2 infection. *BioRxiv*.
- 677 Mizutani, T., Fukushi, S., Iizuka, D., et al. 2006. Inhibition of cell proliferation by SARS-CoV
678 infection in Vero E6 cells. *FEMS Immunology and Medical Microbiology* 46(2), pp. 236–243.
- 679 Oberfeld, B., Achanta, A., Carpenter, K., et al. 2020. SnapShot: COVID-19. *Cell* 181(4), pp.
680 954-954.e1.
- 681 Orchard, S., Ammari, M., Aranda, B., et al. 2014. The MIntAct project - IntAct as a common
682 curation platform for 11 molecular interaction databases. *Nucleic Acids Research*
683 42(Database issue), pp. D358-63.

- 684 Paull, E.O., Carlin, D.E., Niepel, M., Sorger, P.K., Haussler, D. and Stuart, J.M. 2013.
685 Discovering causal pathways linking genomic events to transcriptional states using Tied
686 Diffusion Through Interacting Events (TieDIE). *Bioinformatics* 29(21), pp. 2757–2764.
- 687 Pavlopoulos, G.A., Wegener, A.-L. and Schneider, R. 2008. A survey of visualization tools
688 for biological network analysis. *BioData mining* 1, p. 12.
- 689 Pfaender, S., Mar, K.B., Michailidis, E., et al. 2020. LY6E impairs coronavirus fusion and
690 confers immune control of viral disease. *BioRxiv*.
- 691 R Core Team 2013. *R: A language and environment for statistical computing*. Vienna,
692 Austria: R Foundation for Statistical Computing.
- 693 Sallard, E., Lescure, F.-X., Yazdanpanah, Y., Mentre, F. and Peiffer-Smadja, N. 2020. Type
694 1 interferons as a potential treatment against COVID-19. *Antiviral Research* 178, p. 104791.
- 695 Schubert, M., Klinger, B., Klünemann, M., et al. 2018. Perturbation-response genes reveal
696 signaling footprints in cancer gene expression. *Nature Communications* 9(1), p. 20.
- 697 Shannon, P., Markiel, A., Ozier, O., et al. 2003. Cytoscape: a software environment for
698 integrated models of biomolecular interaction networks. *Genome Research* 13(11), pp.
699 2498–2504.
- 700 Shi, Y., Tan, M., Chen, X., et al. 2020. Immunopathological characteristics of coronavirus
701 disease 2019 cases in Guangzhou, China. *medRxiv*.
- 702 Su, G., Morris, J.H., Demchak, B. and Bader, G.D. 2014. Biological network exploration with
703 Cytoscape 3. *Current Protocols in Bioinformatics* 47, pp. 8.13.1-24.
- 704 Tsoi, H., Li, L., Chen, Z.S., Lau, K.-F., Tsui, S.K.W. and Chan, H.Y.E. 2014. The SARS-
705 coronavirus membrane protein induces apoptosis via interfering with PDK1-PKB/Akt
706 signalling. *The Biochemical Journal* 464(3), pp. 439–447.
- 707 Türei, D., Korcsmáros, T. and Saez-Rodriguez, J. 2016. OmniPath: guidelines and gateway
708 for literature-curated signaling pathway resources. *Nature Methods* 13(12), pp. 966–967.
- 709 UniProt Consortium 2019. UniProt: a worldwide hub of protein knowledge. *Nucleic Acids*
710 *Research* 47(D1), pp. D506–D515.
- 711 Yu, G. and He, Q.-Y. 2016. ReactomePA: an R/Bioconductor package for reactome pathway
712 analysis and visualization. *Molecular Biosystems* 12(2), pp. 477–479.
- 713 Yu, G., Wang, L.-G., Han, Y. and He, Q.-Y. 2012. clusterProfiler: an R package for
714 comparing biological themes among gene clusters. *Omics: a journal of integrative biology*
715 16(5), pp. 284–287.
- 716 Zhang, H., Ai, J.-W., Yang, W., et al. 2020. Metatranscriptomic Characterization of COVID-
717 19 Identified A Host Transcriptional Classifier Associated With Immune Signaling. *Clinical*

718 *Infectious Diseases.*

719 Zhou, Y., Hou, Y., Shen, J., Huang, Y., Martin, W. and Cheng, F. 2020. Network-based drug

720 repurposing for novel coronavirus 2019-nCoV/SARS-CoV-2. *Cell discovery* 6, p. 14.

Figure 1

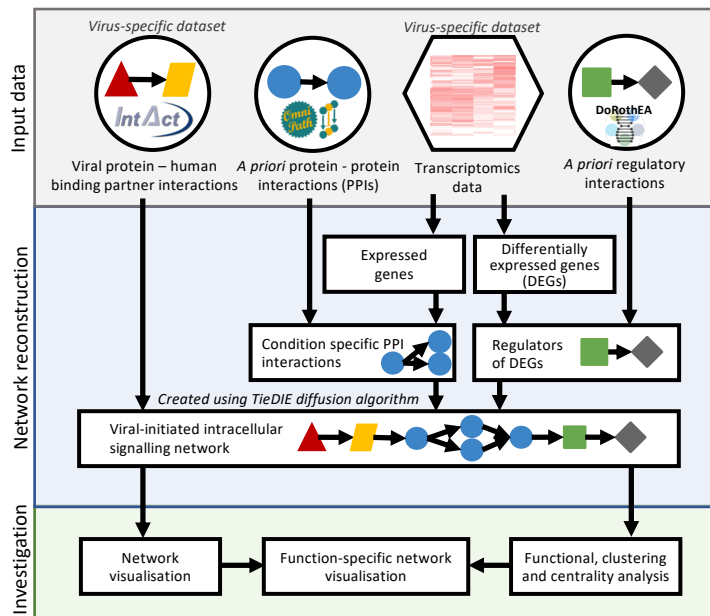
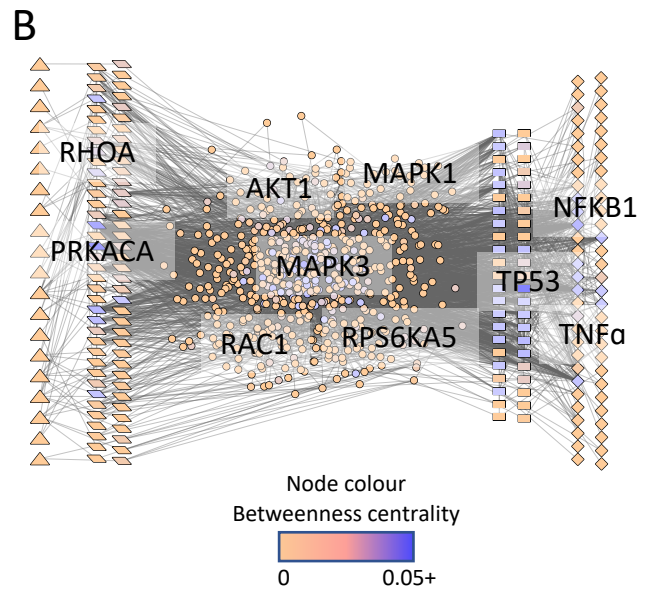
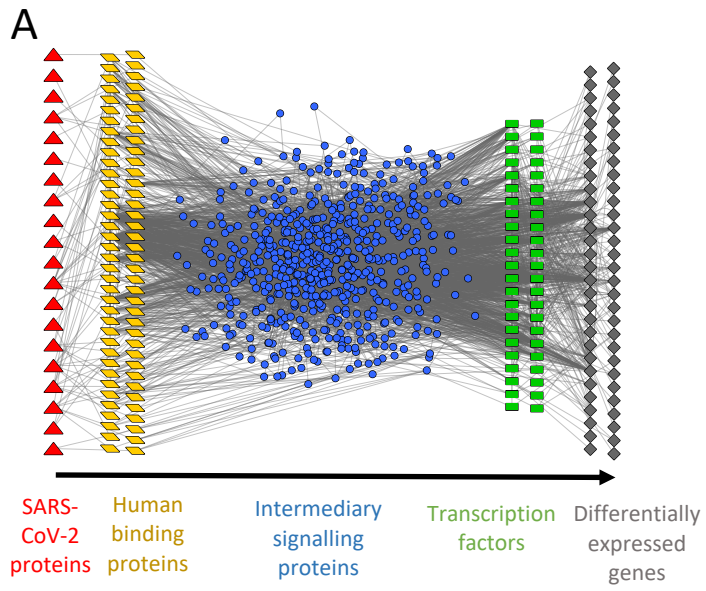
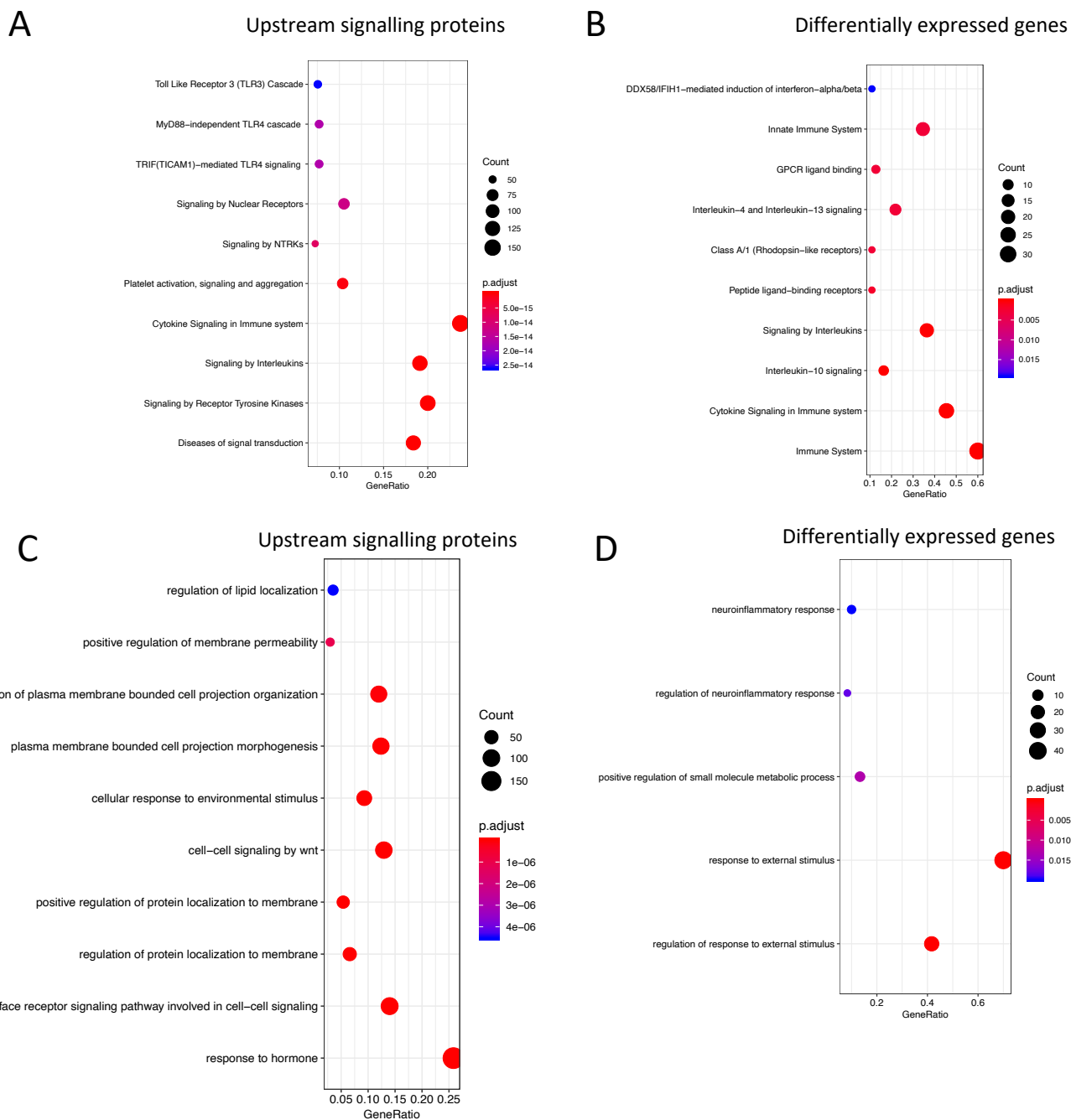


Figure 2

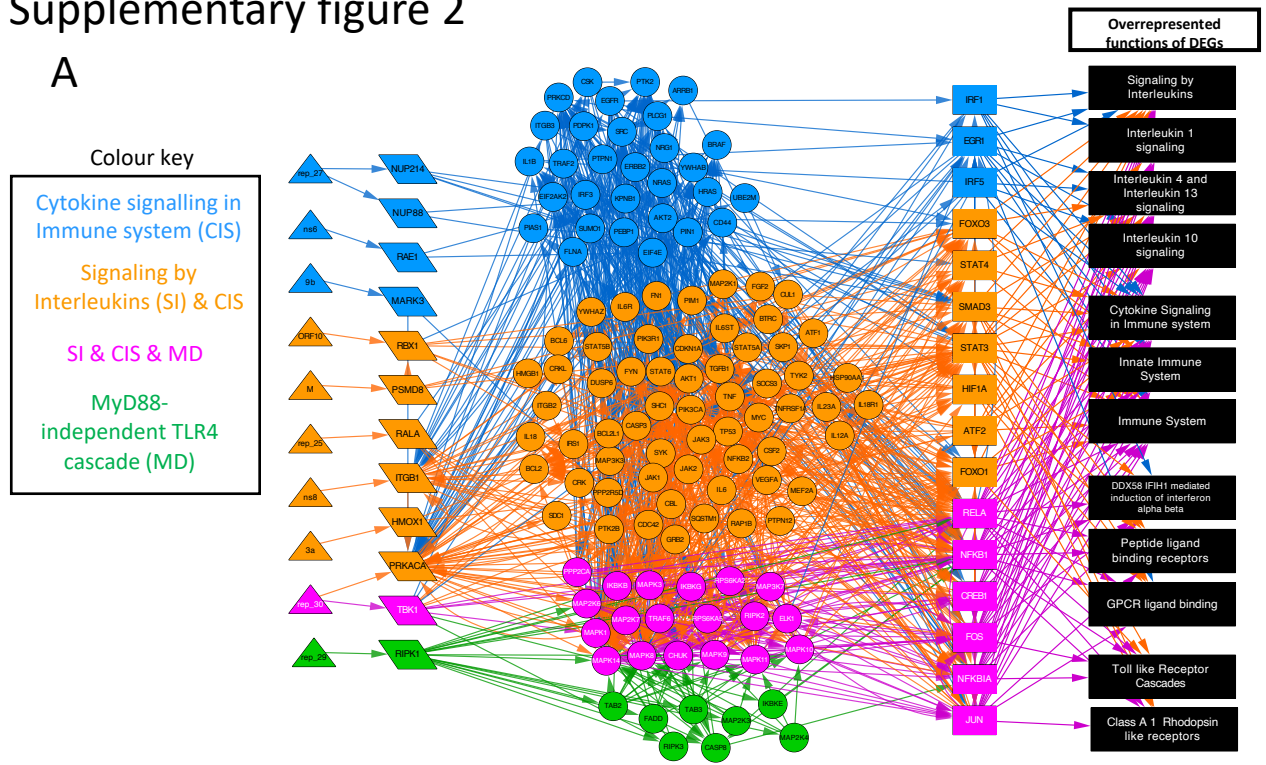


Supplementary figure 1

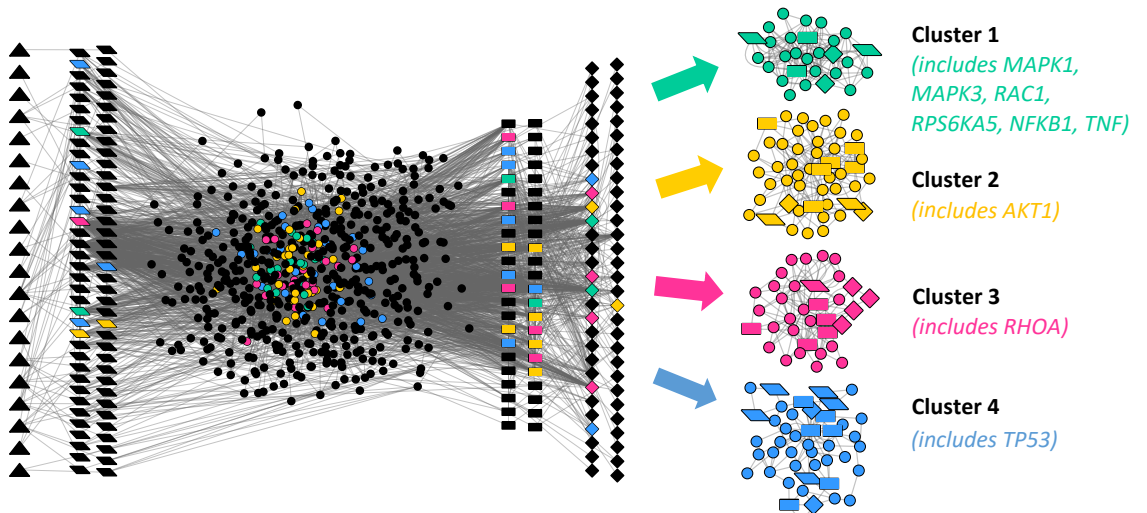


Supplementary figure 2

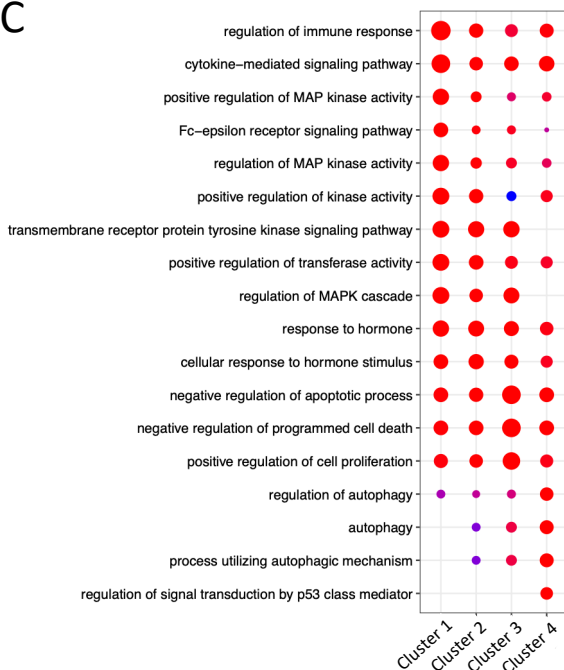
A



B



C



D

